Werk

Jahr: 1977
Kollektion: fid.geo
Signatur: 8 Z NAT 2148:
Digitalisiert: Niedersächsische Staats- und Universitätsbibliothek Göttingen
Werk Id: PPN1015067948_0043
PURL: http://resolver.sub.uni-goettingen.de/purl?PPN1015067948_0043

LOG Id: LOG_0118
LOG Titel: Remote sensing experiment for magnetospheric electric fields parallel to the magnetic field
LOG Typ: article

Übergeordnetes Werk

Werk Id: PPN1015067948
PURL: http://resolver.sub.uni-goettingen.de/purl?PPN1015067948
OPAC: http://opac.sub.uni-goettingen.de/DB=1/PPN?PPN=1015067948

Contact

Niedersächsische Staats- und Universitätsbibliothek Göttingen
Georg-August-Universität Göttingen
Platz der Göttinger Sieben 1
37073 Göttingen
Germany
Email: gdz@sub.uni-goettingen.de

J. Geophys. 43, 731 – 750, 1977

Journal of Geophysics

Remote Sensing Experiment for Magnetospheric Electric Fields Parallel to the Magnetic Field

K. Wilhelm

Max-Planck-Institut für Aeronomie, D-3411 Katlenburg-Lindau 3, Federal Republic of Germany

Abstract. Taking the indications of field-aligned electric fields occurring in the magnetosphere as point of departure and considering the consequences of these fields for magnetospheric dynamics, this paper discusses a remote sensing experiment for magnetospheric electric fields parallel to the magnetic field. The concept of the experiment requires that test particles are artificially injected into the magnetosphere from some appropriate spacecraft. Under suitable conditions the particles will be reflected and be observable as fast echoes. Means of observing these echoes are discussed with particular emphasis on the observation of the transit times as functions of the magnetic moment and of the energy. The transit time function is also theoretically obtained by integrating the equation of motion of the guiding centre of a test particle. It is shown that this function distinctly differs for different electric field configurations. By solving Abel's integral equation, the electric field along the magnetic field line can approximately be reconstructed from the transit time observations for certain configurations. It is concluded that this method is capable of providing structural information on $E_{\parallel}B$-regions in the magnetosphere using rather general model assumptions.

Key words: Magnetospheric electric fields – Field-aligned electric fields – Fast electron echoes.

1. Introduction

The Earth's magnetic field provides a framework for the structure of the various ionized particle populations forming the magnetosphere. The lack of adequate experimental techniques for static electric field observations in this region led to an underestimate of the importance of electric fields for magnetospheric dynamical processes. Although theoretical considerations suggested the decisive rôle of the electric field perpendicular to the magnetic field, the understanding was hampered by the ignorance on the distribution of these fields and their

projection along the magnetic field lines. One school of thought claimed that magnetic field lines should be equipotentials and therefore only the electric field component perpendicular to the magnetic field should be of any significance. Alfvén (1958), however, had pointed out that electric fields parallel to the magnetic field should exist in the magnetosphere. It is clear that these electric fields would have a major impact on energetic particle acceleration and precipitation.

There also is experimental evidence now available that field-aligned electric fields are present in and above the ionosphere at least occasionally. A detailed review on parallel electric fields has recently been given by Mozer (1976). Double-probe observations on sounding rockets have indicated that parallel electric fields of the order of 10 to 20 mV/m are present in the lower magnetosphere (Mozer and Bruston, 1967; Kelley et al., 1971). Energetic particle precipitation with nearly monoenergetic fluxes has been observed on many occasions and has often been interpreted as being caused by parallel electric field acceleration (Albert, 1967; Evans, 1968; Westerlund, 1969; Choy et al., 1971; Reasoner and Chappell, 1973; Arnoldy et al., 1974). These measurement have furthermore shown that the maximum potential drop along a field line is of the order of 10 to 15 kV, as the energy at which these monoenergetic peaks occur consistently lies below this value. With the assumption that electrons moving up the field line are reflected by the parallel electric field region and thus added to the original monoenergetic spectrum Evans (1974) has reached a good agreement between the spectral observations and his model. These interpretations are also consistent with the observations of inverted-V structures in the auroral energetic particle spectrogrammes (Frank and Ackerson, 1971). Field-aligned electron and proton fluxes have also been observed and interpreted as a consequence of parallel electric field acceleration near the ionosphere, although other processes cannot completely be ruled out (Hoffman and Evans, 1968; Hultqvist, 1971; Choy et al., 1971; Whalen and McDiarmid, 1972; Evans et al., 1972; Bosqued et al., 1974; Arnoldy et al., 1974). The observation that artificially injected Barium ions experienced an electrostatic acceleration at several 1000 km altitude has provided strong support for the existence of field-aligned electric fields (Haerendel et al., 1976).

Similar conclusions have been reached by analysing high-time resolution studies of energy dispersion events occurring in energetic particle fluxes (Lampton, 1967; Johnstone and Davis, 1974). Finally the recent observation of the Earth kilometric electromagnetic radiation during substorm events (Gurnett, 1974, 1975) and observations of currents and plasma waves in the disturbed polar cusp (Fredricks et al., 1973) might be indications of turbulent interaction in the lower magnetosphere giving rise to anomalous resistivity and consequently to parallel electric fields.

If only Coulomb collisions are acting, the resistivity of the magnetospheric plasma along the magnetic lines of force should be very small and potential drops can only be maintained by a differential anisotropy of different particle species in a magnetic mirror configuration or by a thermoelectric effect (Hultqvist, 1971; Block and Fälthammar, 1976).

Theoretical arguments (Holzer and Sato, 1973; Fälthammar, 1969; Kindel

and Kennel, 1971; Block, 1972) and laboratory observations (Hamberger and Friedman, 1968), however, suggest that the resistivity of a plasma along the magnetic field increases by orders of magnitude if the current along the line of force reaches a certain threshold. The turbulent region and consequently the electric field would be distributed along the magnetic field line. Another theoretical prediction is that very localized electric double layers form within a distance of 10 to 100 Debye lengths and give rise to steep potential drops. The distinction may be less pronounced as the possibility of many double layers existing simultaneously cannot be ruled out a priori.

In the light of these considerations, the first objective of this experiment would thus be to demonstrate conclusively the existence of parallel electric fields. In order to distinguish between the theoretical interpretations mentioned above, or possibly still another hypothesis, it is essential to determine the structure of the electric field region along the magnetic field line with good spatial resolution. This implies, in particular, the location of the electric field above the ionosphere and the total potential drop. It is also required to study the latitudinal and longitudinal extent of the electric field regions and the time and conditions of their occurrences.

2. Experiment Concept

The experimental difficulties in measuring magnetospheric electric fields parallel to the magnetic field primarily stem from the following facts:

– The electric fields are very small and thus require for their direct detection very sensitive and accurate measurements.

– Direct measurements can significantly disturb the environment in the rarefied plasma.

– The height region in which parallel electric fields seem to play a rôle can only be investigated by satellites in high-inclination orbits during very short passes and is very difficult or not at all amenable to sounding rocket investigations.

– The satellite observations can in any case not provide height profiles, whereas the sounding rocket investigations can at best only be done sporadically.

– The spacecraft motion introduces $\mathbf{v} \times \mathbf{B}$-contributions into the electric field measurements that can only be taken into account with difficulty.

A considerate look at these experimental difficulties suggests employing a remote sensing technique for the investigation of the parallel electric fields. Such a technique could consist of artificially injected energetic particles of different species, e.g. electrons or protons. They subsequently move along the magnetic field line until they are reflected by potential barriers. It will thus be possible to detect the particles near their point of injection as fast echoes and determine their transit time. It will be demonstrated that the method is able to provide profiles of the electric field distribution along the magnetic field line and in addition a value of the total potential drop that is nearly model-independent.

The concept of the experiment is sketched in Figure 1. It has been assumed

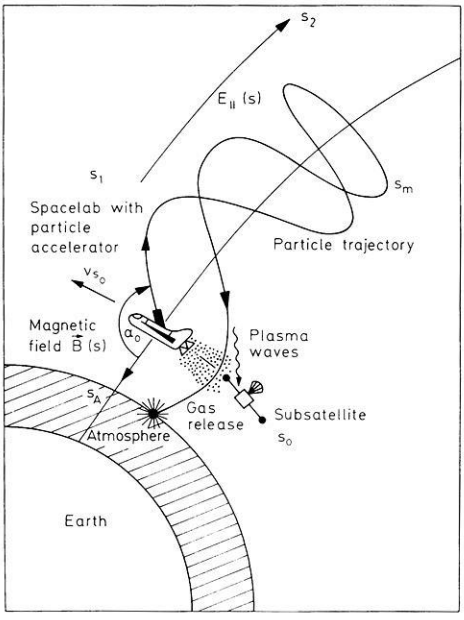

Fig. 1. Conceptual view of the remote sensing experiment for electric fields parallel to the magnetic field. The particles will be injected from a spacecraft at a location s_0 and reflected at s_m within an electric field region extending from s_1 to s_2. The top of the dense atmosphere is denoted by s_A

that the particle injection device is mounted on a Shuttle/Spacelab system. Particles of initial kinetic energy W are being injected at s_0 under a pitch angle of α_0. The parameter s is measured along the magnetic field line with $s=0$ at the Earth's surface. As a first approximation it will be assumed that the particles behave adiabatically, which means that the particle magnetic moment

$$\mu=[W-q\phi(s)]\,B^{-1}(s)\sin^2\alpha(s) \tag{1}$$

with

W initial kinetic energy of particle
q charge of test particle
ϕ electric potential with $\phi(s_0)=0$
B magnetic field strength
α pitch angle

is an invariant of the particle motion. If only static magnetic fields are acting on a particle, the energy of the particle also is constant. In the presence of parallel electric fields this does not hold any longer and the particle energy in the non-relativistic approximation changes as given by

$$m\,(v_{\perp}^2+v_{\parallel}^2)/2=W-q\phi(s) \tag{2}$$

with

m mass of test particle
$v_{\perp}$ transverse velocity with respect to **B**
$v_{\parallel}$ parallel velocity with respect to **B**

Equations (1) and (2) can be combined to give the parallel velocity of the particle guiding centre along the magnetic field

$$v_{\|} = \{2[W - q\phi(s) - \mu B(s)]/m\}^{1/2} \tag{3}$$

For a magnetic dipole configuration the inequality

$$\mu \, dB/ds < 0 \tag{4}$$

holds everywhere below the peak altitude of a given field line. Without electric field it is thus obvious that only bounce motions of the particles between conjugate points can be performed as the parallel velocity is always increasing while the particles are moving up the field lines. Observations of bounce echoes have been made by Winckler (1976) on several occasions and have provided information on the gross magnetic field configuration. The discussion in this paper will be limited to cases where there is an electric field above the ionosphere satisfying the condition

$$\text{sign}\,[q\phi(s)] > 0 \tag{5}$$

which is a necessary but not a sufficient condition for the occurrence of fast echoes. Field reversals as a function of s will not be considered. After injection from either a Shuttle/Spacelab or a rocket system, the particles spiral around the magnetic field line until they are reflected by a potential barrier. Although the particle injection is a rather straightforward procedure, the subsequent detection is much more involved and requires elaborate considerations and possibly rather complex experimental procedures.

The simplest way of finding the reflected particles would be to observe their interaction with the atmosphere. Optical observations should be capable of detecting electron beams with a power of more than 1 kW (Winckler, 1976). These observations could either be done from Spacelab, from the ground or from aircraft. Due to the large observing screen, it would be possible to determine the transit time as a function of the injection parameters. Using this method one would not expect great difficulties from drift displacements of the particles caused by perpendicular electric fields.

The disadvantages of the optical method are first that protons cannot effectively be detected, second that the beam current required is rather high and will probably not fulfill a non-perturbation criterion, and lastly that the optical observations are too indirect to determine energy and pitch angle modifications of the particles that might give a clue to the understanding of the turbulent interaction processes in the lower magnetosphere. In an attempt to avoid high beam currents for optical detection, one might modify the optical method by releasing gas from the space vehicle itself. Successful detection of the injected beam by this method has been reported by Winckler (1976). With releases controlled in time and direction it should thus be possible also to detect the echo beam.

Detailed information on the returning beam can only be obtained by direct observation of the reflected particles. This method suffers from the high orbital velocity of Spacelab. For instance, in a circular orbit passing through $s_0 = 500$ km at a geomagnetic latitutde of 67 deg the orbital velocity is $v_{s_0} = 7.64$ km/s and

the orbital period is $T_{\text{orbit}} = 5.65 \times 10^3$ s. In the guiding centre approximation the injected particle will stay on the field line of injection and consequently the detection device has to be mounted on a spacecraft that will trail Spacelab in such a manner as to be on this field line after the transit time of the test particle. It will be shown later that transit times for electrons vary from 0 to about 1 s consequently requiring separation distances of the subsatellite from the Shuttle/Spacelab system between 0 and 10 km. Moreover, the perpendicular electric field introduces a $\mathbf{E} \times \mathbf{B}$-drift that leads to displacements either parallel or perpendicular to the orbital velocity. If the particles are injected from a sounding rocket, the experiment does not have to cope with a high orbital velocity, however, the unknown $\mathbf{E} \times \mathbf{B}$-drift is still of major concern.

Despite these difficulties the direct detection method is of potential usefulness, in particular, when combined with other methods. This is mainly so because of the fact that by varying the injection parameters energy and pitch angle the return beam can be swept over the particle detector position. Direct measurements have the additional advantage that the required beam intensities are expected to be low and, therefore, should satisfy the non-perturbation criterion.

It must be mentioned at this juncture that the direct detection of reflected particles is even more involved than discussed so far. This derives from the fact that the artificial beam is highly anisotropic as it is laterally confined within one Larmor radius from the injection field line. Contrary to the situation for natural particle flux observations, the azimuth of the detector viewing direction therefore becomes of great importance. Even if the detector is placed at the correct location and is looking under the right pitch angle, it will not be able to see the beam particles unless the detector also looks into the right azimuth. These rather stringent requirements may be relaxed in the case of nonadiabatic motion of the particles. Provided that the particles do not completely forget their history, non-adiabatic processes will thus be very helpful in increasing the detection probability by decreasing the anisotropy and at the same time increasing the beam width. In order to investigate the possible effects in some more detail, variations of the magnetic moment and the energy have been considered during the propagation of the particles.

One result obtained was that energy variations did not play a major rôle. If magnetic moment variations occur coherently, which seems to be a reasonable assumption under anomalous resistivity conditions (Mozer, 1976), it could be shown that this effect has to be taken into account. Out of the many computer test runs that have been performed for arbitrarily chosen pairs of effective collision times and variations of the magnetic moment, three are plotted in Figure 2. They represent typical examples and clearly demonstrate that there is a pronounced focusing effect acting in this configuration, for which a very simple physical explanation can be given: With decreasing magnetic moment μ the reflection point s_m increases and at the same time the parallel velocity $v_{\parallel}$ increases as well and vice versa. The longer (shorter) trajectory as compared to the undisturbed case is therefore compensated to some extent by the higher (lower) velocity. The particle guiding centre will at the same time experience a random walk around the field line of injection.

Finally, the expectation is that particle beams in a plasma should develop

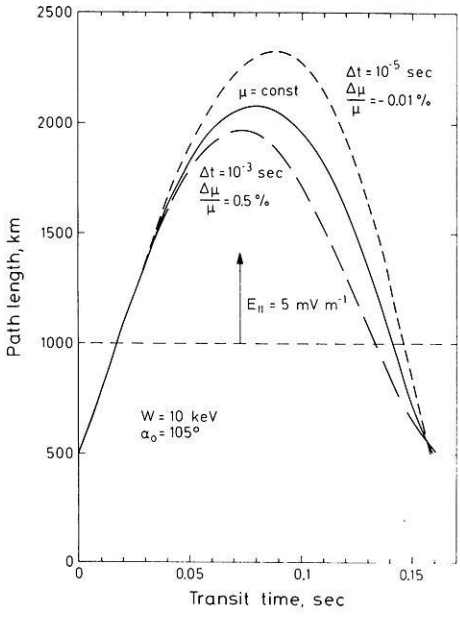

Fig. 2. Modifications of the particle guiding centre trajectory by nonadiabatic effects. The paths of three test particles are plotted over the time elapsed since injection. An electric field region is assumed to be present above $s_1 = 1000$ km with a field strength of 5 mV/m. For two different pairs of the effective collision time and relative variation of the magnetic moment the paths of two particles were evaluated and compared with the particle experiencing no change of the magnetic moment. The effective collision time is defined by the interval in which any interaction of the test particle with its environment leads to a change of the magnetic moment

instabilities that give rise to electrostatic and electromagnetic radiation. Electromagnetic radiation of electron beams injected from sounding rocket payloads have been detected near the plasma frequency (Winckler, 1974). The investigation of the waves emitted by artificially injected particle beams are not only of importance as diagnostic tool but also as a means to study the beam instabilities. Sounding rocket experiments (Hendrickson et al., 1971; Hess et al., 1971; McEntire et al., 1974) have shown that there is no catastrophic instability acting in an artificially injected particle beam so as to prevent subsequent detection, but many plasma waves have been observed at various frequencies.

3. Measurements Required

As has been discussed in Section 2, there are quite a few techniques under study that might eventually be useful for observing the return beam. Any such device or a combination of them must ultimately be capable of performing the following measurements:

– The most important observation of the experiment is the particle transit time as a function of the injection parameters. In this paper we will consider the transit time as a function of the initial energy W and the magnetic moment μ or the initial pitch angle α_0:

$$T = T(W, \mu); \quad 0 \leqq \mu B(s_0) \leqq W. \tag{6}$$

In particular, the dependence on W will be studied while maintaining a constant μ at injection. As the calculated transit times for electrons amount to less

than a second under the assumption of realistic $E_{\parallel}$ B-regions, very high-time resolution observations are required. All candidate methods for obtaining the transit time function have to cope with background problems. As most of the electric field regions can be expected above auroral displays, the optical methods have to eliminate a high natural auroral light background. The wave observations, on the other hand, will have to be carried out with a high background noise resulting from wave-particle interactions of the natural particle fluxes with the ambient wave field. The direct detection method, although handicapped by the orbit and attitude requirements, has the least severe background problem. This is a consequence of the fact that the direct measurements can be done differentially in angle and energy thus reducing substantially the natural flux contributions. If conspicuous reflections of adiabatically behaving particles occur, it can be shown that the ratio of artificially injected to natural electron counts is of the order of 10^4 for an electron beam with currents of approximately 1 mA.

– Also of great importance is the measurement of the total potential drop in the parallel electric field region. This quantity can be observed by determining the energy and magnetic moment thresholds at which the reflection geometry turns over into a transmission configuration. It should be noted that these thresholds are only weakly dependent on the magnetic and electric field model and thus give unambigious information on the electric field properties.

– The measurements of the variations of the initial energy and the modification of the magnetic moment will be of value in studying and understanding the beam-plasma interactions. For the experiment concept developed in this paper these observations are not of primary interest, although a detailed knowledge of the beam-plasma interactions is essential before successful attempts to perform echo identifications can be undertaken.

– The displacement of the beam can be used as a measure of the $\mathbf{E} \times \mathbf{B}$-drift. The particles also experience magnetic gradient and curvature drifts. It can be shown that under auroral conditions the $\mathbf{E} \times \mathbf{B}$-drift is by far the most important drift effect. For the direct detection method it will be helpful to measure the perpendicular electric field by other means and take this information into account when positioning the measuring device, although one has to remember that the field lines will not be equipotentials in the presence of $E_{\parallel}$ fields.

It was already mentioned that this experiment is meant to be a probe experiment. Initially the experiment parameters should therefore be adjusted in such a way as not to disturb or modify the natural conditions leading to the parallel electric field. For an understanding of the physical processes operating above the aurora, it is however also of importance to study the modification of these conditions at a later stage. The essential parameters for these studies obviously are the beam current and power. Under the assumption that the injected beam is confined to a flux tube with a radius of not more than a Larmor radius, the injected energy is comparable to the thermal energy of the natural electrons when the beam current exceeds approximately 10 mA. Hence it is conceivable that modification experiments can be done quite easily.

4. Deductions

A successful preparation of the experiment can only be initiated if the conditions of particle reflection and the expected transit times are well understood. With a view to achieving this goal the following computer simulations of particle motions were performed. In these studies models of the magnetic and electric fields had to be assumed. The magnetic field was approximated by

$$B(s) \sim (s + R_E)^{-3} \tag{7}$$

with R_E being the Earth's radius.

The electric field was assumed to be either constant over a path length of several 1000 km or following a Gaussian distribution along the field line of the form

$$E_{\parallel}(s) = -U(2\pi\sigma^2)^{-1/2} \exp[-(s-\bar{s})^2/2\sigma^2] \tag{8}$$

with

$\bar{s}$ mean value of s
(representative for the location of electric field maximum)
σ^2 variance of s
(representative for width of E-field region)
U potential difference for $s = \pm\infty$.

The equation of the electric field can be integrated to give the potential function

$$\phi(s) = -\int_{s_0}^{s} E_{\parallel}(s)\, ds \tag{9}$$

satisfying the condition $\phi(s_0) = 0$. It is of great importance to note that particles with $\mu > 0$ will not have lost all their kinetic energy at the reflection point. This is a straightforward consequence of the constancy of the magnetic moment in Equation (1) and the Equation (2). As the scattering decreases with increasing particle energy, particles with high transverse energy have a good change to remember their injection and propagation history and will thus be useful for subsequent detection. For a specific electric field configuration the situation is presented in Figure 3. It can be seen that the electric potential at reflection has a minimum for pitch angles of 90° and that after Equation (2) the corresponding kinetic energy has a maximum there. This points to the potential usefulness of particles near 90° pitch angles. There might be a conflict with spacecraft safety requirements as it is clear that these particles will return close to the spacecraft after one Larmor period. In this context one should, however, notice that the required current intensities for this experiment are so low that there is no risk involved, provided the gun can be safeguarded against accidental high-current operation in the 90°-pitch angle direction. Figure 3 also shows that the experiment can utilize pitch angles below 90°, i.e. particles injected downwards, as long as they do not reach the dense atmosphere before being reflected in the magnetic mirror configuration.

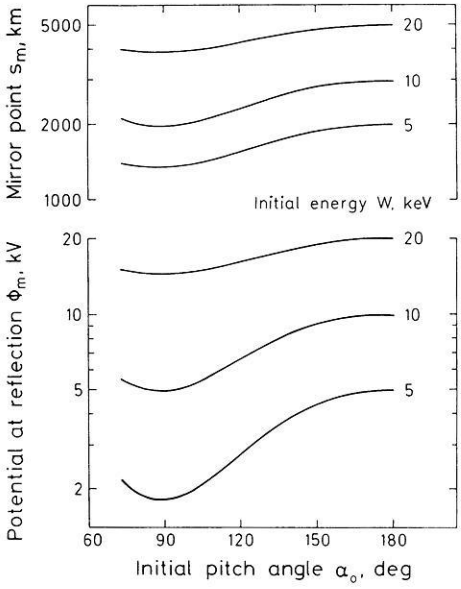

Fig. 3. Electric potential at reflection (lower part) and reflection point (upper part) versus initial pitch angle. Both quantities can be considered as a measure of the penetration depth of the test particles into the electric field layer. The initial kinetic energy W is used as parameter. The electric field model was in this case defined by a constant field of 5 mV/m above $s_1 = 1000$ km

Taking into account the potential drops so far observed in the magnetosphere, one can conclude from Figure 3 that particles of more than 15 keV initial energy will not be very attractive for this experiment as they probably will not be reflected under natural conditions. In the upper part of Figure 3 the reflection point s_m is plotted as a function of the injection pitch angle and with initial energy as parameter. If we restrict the initial energies to values smaller than 15 keV, a path length up to approximately 4000 km can be studied by the experiment in this particular example. It can, however, be said that this range amenable to investigations by this method is typical for most of the configurations considered in this paper.

Using Equation (3) the transit time of the particles can be obtained by integrating the differential times along a given path increment ds according to

$$T = 2 \int_{s_0}^{s_m} v_{\parallel}^{-1} \, ds \tag{10}$$

with

s_m mirror point defined by $v_{\parallel} = 0$.

Numerical integrations of Equation (10) were performed for many different examples. Two of these are shown in Figure 4 in the form

$$T = T(\alpha_0); \quad W = \text{const.} \tag{11}$$

In the upper part of the figure an extended constant electric field has been assumed to exist above the injection point. Particles with high initial energy penetrate deep into this region and consequently have long transit times as compared to low energy particles. If, on the other hand, a double layer configuration with a very localized potential barrier is assumed above the injection point

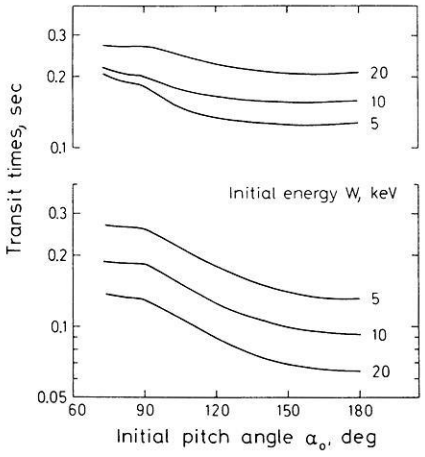

Fig. 4. Transit times of electrons as a function of the initial pitch angle. Calculations were performed for two different models. In the upper part of this figure an extended electric field of 5 mV/m was assumed above $s_1 = 1000$ km. In the lower part an electric double layer configuration at $\bar{s} = 3000$ km was assumed

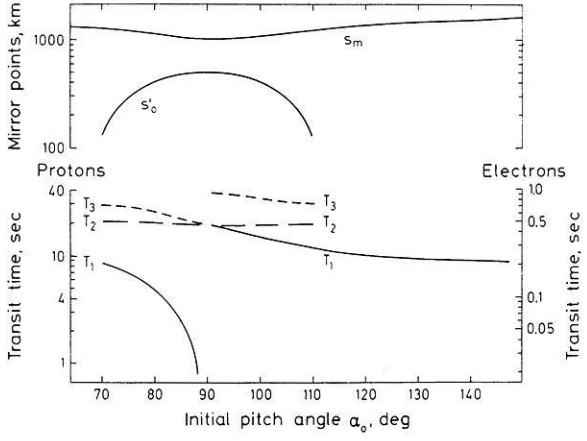

Fig. 5. Transit time calculations for electrons and protons of 1 keV energy as a function of the initial pitch angle α_0 (lower part). Particles outside the local loss cone experience multiple echoes and the relevant transit times are given. The electric field model was characterized by a maximum E-field at $\bar{s} = 3000$ km and a width of the field distribution of ± 1000 km. Mirror points are shown in the upper part

as has been done in the lower part of Figure 4, the length of the trajectory of the guiding centre does not depend critically on the particle energy and therefore particles with high energy need a smaller transit time. This leads to the important conclusion that a distinction between extended and localized electric field regions can unambigiously be made by simply comparing transit times of particles with different injection energies.

In Figure 5 transit time calculations are presented for a Gaussian distribution of the electric field along the magnetic field line. Also given in Figure 5 are the reflection points s_m and s'_0.

The plot of the lower reflection point s'_0 emphasizes the rôle of the local particle loss cone geometry. For particles outside the loss cone a magnetic and electric confinement situation is present resulting in the possibility of multiple reflections. In the lower part of Figure 5, the transit times for multiple reflections are calculated and presented with the notation T_1 for the first, T_2 for the second, T_3 for the third reflection. The first reflection of particles injected downwards is not useful for our purposes. The remaining transit time curves

show, however, that electron echoes can be detected in an interval from 0.2 s upwards reaching approximately 1 s for the transit time T_3. This result proves the important fact that direct particle detection is in principle possible by sweeping the return beam over the subsatellite positioned at a specific location with respect to the injection spacecraft by varying the injection parameters. In this case only the pitch angle was modified. Taking into account that in addition the energy can be varied, one clearly sees that the location of the subsatellite is not as a critical requirement as was to be expected.

The interpretation of the observed transit times in terms of a magnetospheric electric field can be carried out by comparing the observed transit time functions with specific model calculations. This method does normally not lead to an unambigious interpretation and it therefore seems to be advantageous to study the possibility of an inversion of the observed transit time functions in analogy to the ionospheric sounding technique and the relevant inversion formalism (cf. Thomas, 1959; Rishbeth and Garriott, 1969). For this purpose it has been assumed for the remaining part of this paper that the initial energy of the test particles is varying and the magnetic moment is constant at injection. It should be mentioned that a similar but more complex inversion procedure could also be formulated for constant energy and variable magnetic moment.

The task at hand thus is finding a solution $\phi(s)$ under the assumption of a magnetic field model $B(s)$. By substituting the potential energy function

$$\omega(s) = q\phi(s) + \mu B(s) \tag{12}$$

in Equation (3) one obtains

$$v_{\parallel} = [2(W-\omega)/m]^{1/2}. \tag{13}$$

Even with the simplifying assumptions made in Equations (7) and (8) the potential energy function has a rather complicated form as can be seen from Figure 6, where ω is plotted versus s. The initial decrease of the function ω reflects

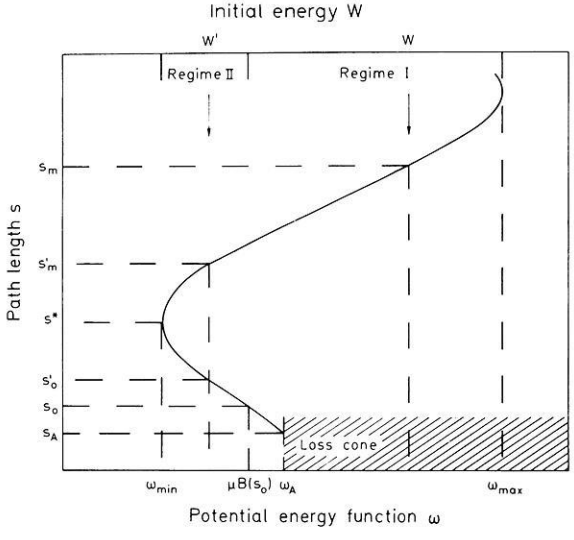

Fig. 6. Typical pattern of the potential energy function ω plotted against s. Two test particles with initial energies W and W' are considered (arrows). The test particle with W' can execute multiple bounce paths between the magnetic and electric mirror configurations. The dividing line between single and multiple echoes is at ω_A corresponding to s_A at the top of the atmosphere

the decrease of the magnetic field with increasing s. After passing a minimum at s^* the function ω increases due to the presence of the electric field until a maximum of ω_{max} is reached. If the electric field is present for very small s the minimum at s^* might disappear in special cases. In order to cope with a more general situation one has to consider that there is no unique solution of $\omega(s)$ in terms of s. Hence it is necessary to define two branches of the solution s. To achieve this, the value of s^* has to be determined by differentiating Equation (12)

$$d\omega/ds = -qE_{\parallel} + \mu dB/ds \tag{14}$$

and considering that ω has to have a minimum at s^*.

Consequently the equation

$$(d\omega/ds)_{s^*} = 0 \tag{15}$$

has to be solved. It is then possible to write the two solutions of s as follows

$$s = \begin{cases} g_1(\omega); & s_0 \leqq s \leqq s^* \\ g_2(\omega); & s^* < s \leqq s_m. \end{cases} \tag{16}$$

The solutions have been restricted to the interval (s_0, s_m) as only there they are of interest for a given energy W at this stage. By differentiating Equation (16) one obtains

$$ds = \begin{cases} g_1'(\omega)\, d\omega; & s_0 \leqq s \leqq s^* \\ g_2'(\omega)\, d\omega; & s^* < s \leqq s_m. \end{cases} \tag{17}$$

In evaluating the importance of Figure 6 one has to remember that the injection point is fixed at s_0. Satisfying $\mu = \text{const}$, only energies $W \geqq \mu B(s_0)$ can be injected there. The necessity to define two solutions s in Equation (16), however, also requires to consider energies below this value. This constitutes the need to distinguish between two regimes defined as follows

$$\begin{aligned} &\text{Regime I:} \quad \mu B(s_0) \leqq \omega, \; W \leqq \omega_{max} \\ &\text{Regime II:} \quad \omega_{min} \leqq \omega, \; W < \mu B(s_0). \end{aligned} \tag{18}$$

With this definition, the Equation (10) can be rewritten and complemented to give

$$T(W)/2 = \begin{cases} \int_{s_0}^{s^*} v_{\parallel}^{-1} ds + \int_{s^*}^{s_m} v_{\parallel}^{-1} ds & \text{if } W \text{ in regime I} \\ \int_{s_0}^{s^*} v_{\parallel}^{-1} ds + \int_{s^*}^{s_m} v_{\parallel}^{-1} ds & \text{if } W \text{ in regime II.} \end{cases} \tag{19}$$

Depending on whether

$$(d\omega/ds)_{s_0} < 0 \tag{20}$$

or

$$(d\omega/ds)_{s_0} \geqq 0 \tag{21}$$

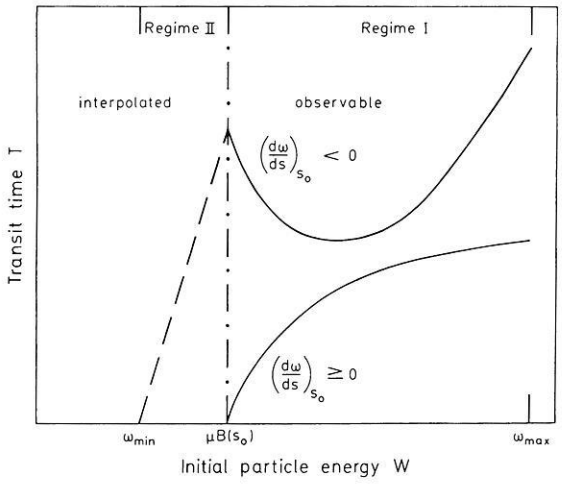

Fig. 7. Transit times as function of the initial particle energy. The upper curve corresponds to the situation where the electric field region is far above the ionsophere. The right-hand portion of this curve in regime I is observable from a space vehicle located at s_0. The part in regime II is not measurable from that location and will be discussed in the text in some detail. The lower curve represents a typical example of a transit time function if an electric field is present in the ionosphere

is valid, the transit time functions show a characteristic difference at $\mu B(s_0)$ that can be formulated by

$$T[\mu B(s_0)] > 0 \tag{22}$$

$$T[\mu B(s_0)] \approx 0 \tag{23}$$

and is also indicated in Figure 7. The physical interpretation of this difference is that in the case of a finite transit time for an energy $W = \mu B(s_0)$ the electric field is located far above the injection point, whereas in the other case the electric field is extending down to the injection point. If the electric field near the injection point is very strong corresponding to the case $(d\omega/ds)_{s_0} \gg 0$ even particles with energies $W = \mu B(s_0)$ will be driven down into the atmosphere and be lost for our purpose. The distinct difference between those two cases should substantially facilitate the observational determination of whether the electric field region is far above or very near the ionosphere.

Equations (13), (17) and (19) can be combined to give

$$T(W) = (2m)^{1/2} \int_{\omega_{min}}^{W} [g_2'(\omega) - g_1'(\omega)] (W - \omega)^{-1/2} \, d\omega \tag{24}$$

if we define $g_1'(\omega) \equiv 0$ for all ω in regime I. This definition is appropriate as it means that the transit time is reckoned from and to the injection point. There are several interesting features to note about Equation (24):

– It directly follows from physical arguments that $T(\omega_{min}) = 0$ as at this location the particle is situated at the bottom of the potential well.

– At $\mu B(s_0)$ the function T is not differentiable because of the sudden disappearance of the branch $g_1(\omega)$. The physical interpretation is that in regime I only the upper mirror process is contributing to the transit time. The discontinuity is of course not present if the potential function has no minimum for specific electric field configurations.

– It is known as Abel's integral equation. Solutions exist under the condition that $T(W)$ is continuously differentiable.

Hence it can be concluded that exact inversions of the measured transit time function can be carried out if an sizable electric field reaches down to the ionosphere. In those cases where the electric field region is high above the ionosphere, there are two problems to be considered before a suitable inversion procedure can be performed.

The first problem was already mentioned and is related to the fact that the transit time function can only be observed for initial energies greater than $\mu B(s_0)$, i.e. in regime I. The transit time function in regime II can in principle be measured by raising the injection point starting from s_0 to s^*. There is of course no possibility to do so on an orbiting spacecraft because of the gravitational law, but a high-altitude sounding rocket could eventually be a suitable carrier for such an experiment. Considering that with the assumptions made in Equations (7) and (8) the transit time can only monotonously decrease while s is increasing from s_0 to s^* and that $T(\omega_{\min})=0$, one is even able to produce a good interpolation without measurements, for instance, by assuming a linear relationship. The second problem is that the condition of $T(W)$ being a continuously differentiable function is not always fulfilled. As we are discussing physical processes rather than mathematical concepts, it seems feasible to introduce suitable smoothing functions so as to ensure the required continuity without significantly influencing the physical consequences. A detailed discussion is however beyond the scope of this study. It was thought that the easiest way to demonstrate the range of application was to numerically analyse three examples and see whether the results are acceptable approximations of the original electric field configuration.

The solution of Abel's integral equation can be found in textbooks (e.g. Schlögl, 1956) and can be written in the form

$$g_2'(\omega)\,d\omega - g_1'(\omega)\,d\omega = (2m\pi^2)^{-1/2}\,d\int_{\omega_{\min}}^{\omega} T(W)(\omega - W)^{-1/2}\,dW. \tag{25}$$

Taking into account Equation (17), the integration of Equation (25) yields

$$\left.\begin{array}{ll} \text{for } \omega \text{ in regime I} & s - s_0 \\ \text{and in regime II} & s - s_0' \end{array}\right\} = (2m\pi^2)^{-1/2} \int_{\omega_{\min}}^{\omega} T(W)(\omega - W)^{-1/2}\,dW \tag{26}$$

giving the path s as a function of ω. Using Equation (12) and inserting the magnetic field at s, one can obtain the potential $\phi(s)$. Differentiation then leads to the electric field as a function of s. It should be noted that Equation (26) is only useful if ω lies in regime I as in regime II the contribution of s and s_0' cannot easily be distinguished. Fortunately, it is regime I that is of interest, because there the electric field influence becomes of significance. One should also remember that in general no observations will be available in regime II.

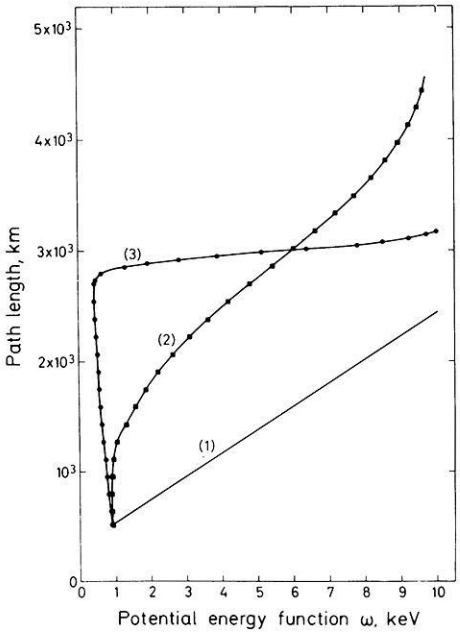

Fig. 8. Potential energy function versus s for three examples of electric field distributions

Incidentically it should be mentioned that Equation (24) can be extended by a suitable continuation of $g_1'(\omega) \neq 0$ in regime I:

$$T^*(W) = (2m)^{1/2} \int_{\omega_{min}}^{W} [g_2'(\omega) - g_1'(\omega)](W-\omega)^{-1/2}\, d\omega; \quad \omega_{min} \leqq W < \omega_A \tag{27}$$

with

$$\omega_A = \omega(s_A)$$

and

$$T^*(\omega_{min}) = 0.$$

It can be seen from Figure 6 that the interval defined by $\omega_{min} \leqq W \leqq \omega_A$ corresponds to the region where multiple echoes between the magnetic and the electric mirror configuration are possible. The transit time T^* thus corresponds to one total bounce path and is the increment of the multiple-echo transit time.

In the first example to be presented an electric field of 5 mV/m has been assumed to extend from the ionosphere upwards. The potential energy function is given as curve 1 in Figure 8. It can be seen that in this case there is no minimum of $\omega(s)$. One can thus expect that an exact solution of Abel's integral equation will be possible. The corresponding transit time function is plotted in the lower part of Figure 9 as curve 1. The reflection point as a function of energy is shown in the upper part of Figure 9 again labelled with 1 for this particular case. The next example is representative for an extended electric field region far above the ionosphere. A Gaussian distribution of the field

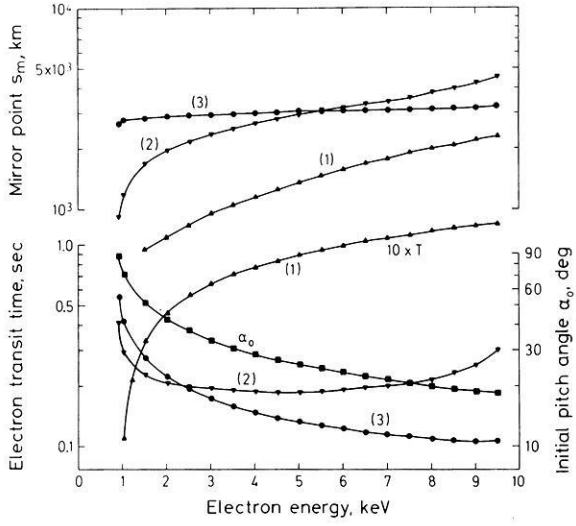

Fig. 9. Electron transit time curves are plotted as a function of the initial electron energy for the three examples along with the corresponding reflection points. Note that the transit times for example 1 are multiplied by a factor of 10 in order to adjust the scale. Also given is the initial pitch angle that is identical for all three examples

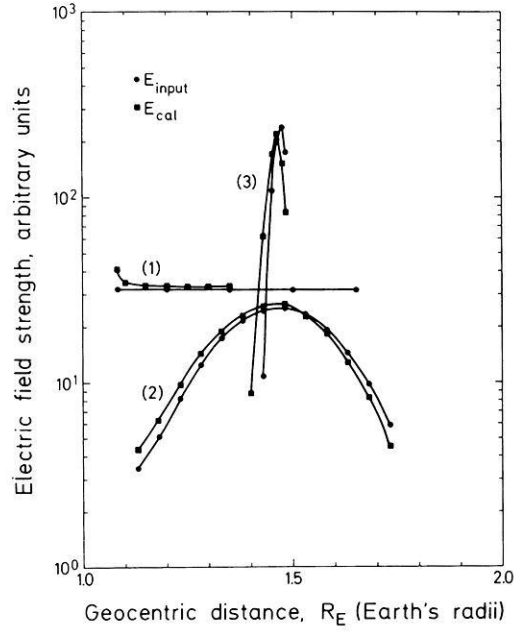

Fig. 10. Comparison of the theoretical electric field strengths as a function of geocentric distance with the calculated electric fields for three different model assumptions

has been assumed with the location of the maximum value at $\bar{s}=3000$ km and a width of $\pm$ 1000 km. Again the potential energy function is given in Figure 8 (curve 2). Results of the transit time and the reflection point calculations are depicted in Figure 9 and labelled appropriately. The last model has been adjusted to fit a double layer configuration. The assumptions of a Gaussian distribution of the electric field and the location of the maximum value are identical to those in example 2, but the width of the electric field region is

decreased to ± 10 km. The potential energy function ω is plotted as graph 3 in Figure 8 and the reflection point and transit time curves can be found in Figure 9.

A comparison between the model assumptions and the results of the inversion process can best be made by comparing the calculated field with the theoretical input field. This is done for all three examples in Figure 10. As was to be expected, the input and the calculated fields agree reasonably well for example 1, where the transit time function is continuously differentiable and thus fulfills the requirement for an exact inversion. The discrepancy revealed at low altitudes results from calculation inaccuracies due to the finite integration intervals near the reflection point. The other two cases, where the inversion conditions are not fulfilled, clearly show that there are differences between the input and the output electric fields. However, the differences are small and moreover the values and the locations of the maximum fields are so similar in both cases that one has to conclude that this method is adequate for approximating the inversion problem for a variety of electric field configurations with sufficient accuracy. When calculating the electric field, the exact transit time functions $T(W)$ in both regimes have been employed here. The use of interpolations in regime II will result in additional complications as discussed earlier. The discussion have been restricted to relatively simple electric field configurations. More complicated situations, e.g. with more than one significant electric field region, will normally lead to discontinuous transit time functions that cannot unambiguously be inverted.

5. Conclusions

In view of the importance of the electric field parallel to the magnetic field for an understanding of the magnetospheric dynamics, a major effort is justified to investigate this phenomenon. At the same time, the plasma physical processes can be studied that are responsible for maintaining a substantial parallel electric field. Compared to other methods such as Barium shaped-charge injections and double-probe measurements that both have provided evidence on the existence of parallel electric fields, the use of electron and proton beams as tracers of the electric field configuration seems to offer several advantages. At this stage it is not possible to clearly demonstrate the feasibility of the tracer experiment. However, there is such a variety of possibilities inherent in this experiment that there is little doubt that a careful approach will lead to a successful investigation of parallel electric fields by this method. Early investigations can be performed on sounding rocket payloads. The small velocity of a rocket perpendicular to the magnetic field is a significant advantage over any orbiting system. Sounding rocket studies in this field suffer, however, from the constraint that no comprehensive study in time and geographic location can be conducted and that the measuring modes normally have to be preprogrammed thus rendering the instrument rather inflexible during flight.

The Shuttle/Spacelab System will offer many improvements over conventional spacecraft in this context. First of all a systematic study on a worldwide

scale can be carried out with a view to determining the magnetosphere-ionosphere coupling. The high payload carrying capability of the system will also make possible integrated studies of all the relevant parameters. In particular the perpendicular electric field at the location of the Shuttle/Spacelab System can be determined and will be of use in positioning manoeuvrable subsatellites if those are available for this type of study. The combination of optical and direct detection methods hopefully supported by wave experiments will eventually yield complete information on the transit time functions and thus gives the necessary input parameters for the inversion problem.

Acknowledgements. I thank Drs. W. Bernstein, G. Kremser and W. Stüdemann for many stimulating discussions on this topic. Dr. H.J. Müller's and Mr. F. Both's assistance in performing the numerical calculations is greatly acknowledged. This investigation was supported by the German Bundesministerium für Forschung und Technologie under grants No. WRT 1074 and WRK 274/3.

References

Albert, R.D.: Energy and flux variations of nearly monoenergetic auroral electrons, J. Geophys. Res., **72**, 5811–5815, 1967

Alfvén, H.: On the theory of magnetic storms and aurorae, Tellus, **10**, 104–116, 1958

Arnoldy, R.L., Lewis, P.B., Isaacson, P.O.: Field-aligned auroral electron fluxes, J. Geophys. Res., **79**, 4208–4221, 1974

Block, L.P.: Acceleration of auroral particles by electric double layers, in Earth's Magnetospheric Processes (B.M. McCormac, ed.) D. Reidel Publ. Comp., Dordrecht-Holland, pp. 258–267, 1972

Block, L.P., Fälthammar, C.-G.: Mechanisms that may support magnetic-field-aligned electric fields in the magnetosphere, Ann. Geophys., **32**, 161–174, 1976

Bosqued, J.M., Cardona, G., Rème, H.: Auroral electron fluxes parallel to the geomagnetic field lines, J. Geophys. Res., **79**, 98–104, 1974

Choy, L.W., Arnoldy, R.L., Potter, W., Kintner, P., Cahill, L.J., Jr.: Field-aligned particle currents near an auroral arc, J. Geophys. Res., **76**, 8279–8298, 1971

Evans, D.S.: The observations of a near monoenergetic flux of auroral electrons, J. Geophys. Res., **73**, 2315–2323, 1968

Evans, D.S.: Precipitating electron fluxes formed by a magnetic field-aligned potential difference, J. Geophys. Res., **79**, 2853–2858, 1974

Evans, D.S., Maehlum, B., Wedde, T.: High latitude observations of field-aligned electron beams (Abstract), Trans. Am. Geophys. Union, **53**, 731, 1972

Fälthammar, C.-G.: Fundamental electromagnetic processes in the outer magnetosphere, in Atmospheric Emissions (B.M. McCormac and A. Omholt, eds.), pp. 37–46, New York: Van Nostrand Reinhold Comp., 1969

Frank, L.A., Ackerson, K.L.: Observations of charged particle precipitation into the auroral zone, J. Geophys. Res., **76**, 3612–3643, 1971

Fredricks, R.W., Scarf, F.L., Russell, C.T.: Field-aligned currents, plasma waves, and anomalous resistivity in the disturbed polar cusp, J. Geophys. Res., **78**, 2133–2141, 1973

Gurnett, D.A.: The Earth as a radio source: Terrestrial kilometric radiation, J. Geophys. Res., **79**, 4227–4238, 1974

Gurnett, D.A.: The Earth as a radio source: The nonthermal continuum, J. Geophys. Res., **80**, 2751–2763, 1975

Haerendel, G., Rieger, E., Valenzuela, A., Föppl, H., Stenbaek-Nielsen, H.C., Wescott, E.M.: First observation of electrostatic acceleration of Barium ions into the magnetosphere, Proceedings of the symposium on European programmes on sounding-rocket and balloon research in the auroral zone, ESA SP **115**, 203–211, 1976

Hamberger, S.M., Friedman, M.: Electrical conductivity of a highly turbulent plasma, Phys. Rev. Lett., **21**, 674–677, 1968

Hendrickson, R.A., McEntire, R.W., Winckler, J.R.: Electron echo experiment: A new magnetospheric probe, Nature, **230**, 564–566, 1971

Hess, W.N., Trichel, M.C., Davis, T.N., Beggs, W.C., Kraft, G.E., Stassinopoulos, E., Maier, E.J.R.: Artificial aurora experiment: Experiment and principal results, J. Geophys. Res., **76**, 6067–6081, 1971

Hoffman, R.A., Evans, D.S.: Field-aligned electron bursts at high latitudes observed by OGO 4, J. Geophys. Res., **73**, 6201–6214, 1968

Holzer, T.E., Sato, T.: Quiet auroral arcs and electrodynamic coupling between the ionosphere and the magnetosphere, 2, J. Geophys. Res., **78**, 7330–7339, 1973

Hultqvist, B.: On the production of a magnetic-field-aligned electric field by the interaction between the hot magnetospheric plasma and the cold ionosphere, Planetary Space Sci., **19**, 749–759, 1971

Johnstone, A.D., Davis, T.N.: Low-altitude acceleration of auroral electrons during breakup observed by a mother-daughter rocket, J. Geophys. Res., **79**, 1416–1425, 1974

Kelley, M.C., Mozer, F.S., Fahleson, U.V.: Electric fields in the nighttime and daytime auroral zone, J. Geophys. Res., **76**, 6054–6066, 1971

Kindel, J.M., Kennel, C.F.: Topside current instabilities, J. Geophys. Res., **76**, 3055–3078, 1971

Lampton, M.: Daytime observations of energetic auroral-zone electrons, J. Geophys. Res., **72**, 5817–5823, 1967

McEntire, R.W., Hendrickson, R.A., Winckler, J.R.: Electron echo experiment I: Comparison of observed and theoretical motion of artificially injected electrons in the magnetosphere, J. Geophys. Res., **79**, 2343–2354, 1974

Mozer, F.S.: Anomalous resistivity and parallel electric fields, in Magnetospheric particles and fields, (B.M. McCormac, ed.) D. Reidel Publ. Comp., Dordrecht-Holland, pp. 125–136, 1976

Mozer, F.S., Bruston, P.: Electric field measurements in the auroral ionosphere, J. Geophys. Res., **72**, 1109–1114, 1967

Reasoner, D.L., Chappell, C.R.: Twin payload observations of incident and backscattered auroral electrons, J. Geophys. Res., **78**, 2176–2186, 1973

Rishbeth, H., Garriott, O.K.: Introduction to ionospheric physics, New York-London: Academic Press 1969

Schlögl, F.: Randwertprobleme, in: Handb. Phys., Bd. 1, (S. Flügge, ed.) Berlin-Göttingen-Heidelberg: Springer, pp. 218–352, 1956

Thomas, J.O.: The distribution of electrons in the ionosphere, Proc. I.R.E., **47**, 162–175, 1959

Whalen, B.A., McDiarmid, I.B.: Observations of magnetic-field-aligned auroral electron precipitation, J. Geophys. Res., **77**, 191–202, 1972

Westerlund, L.H.: The auroral electron energy spectrum extended to 45 eV, J. Geophys. Res., **74**, 351–354, 1969

Winckler, J.R.: An investigation of wave-particle interactions and particle dynamics using electron beams injected from sounding rockets, Space Sci. Rev., **15**, 751–780, 1974

Winckler, J.R.: A summary of recent results under the 'Echo' program for the study of the magnetosphere by artificial electron beams, Report, School of Physiscs and Astronomy, Univ. Minnesota, Minneapolis, 1976

Received December 17, 1976; Revised Version May 9, 1977